

MAGNUS AND DRAG FORCES ACTING ON GOLF BALL

A. Kharlamov, Z. Chara, P. Vlasak
Institute of Hydrodynamics AS CR, v.v.i., Prague

Abstract

The paper describes the results of experiments with a rotating golf ball moving quasi-steadily in calm water. The motion of the ball was recorded on a digital video camera. The Cartesian coordinates and the angle of rotation of the ball were determined from the records of motion. The dimensionless drag force coefficient, Magnus force coefficient and translational and rotational Reynolds numbers were calculated from the time series of the ball coordinates and the angle of rotation for each recorded frame. The calculated data were averaged over rectangular cells on experimental domain on the plane of translational and rotational Reynolds numbers, i.e. $1.2 \cdot 10^4 < Re < 1.6 \cdot 10^4$ and $3.8 \cdot 10^3 < Re_\omega < 2.7 \cdot 10^4$.

Introduction

The investigation of aerodynamic forces on rugged spheres is mostly connected with ball games. In such games as baseball, golf, football, and cricket, the lateral deflection of a rotating ball is of great interest for the player. In golf the rotation of the ball allows to obtain the higher and longer trajectories; in football the spinning of the ball allows to score from zones, from which it would be impossible to score without spinning. The lateral deflection of a ball is caused by the lateral force due to simultaneous rotational and translational movement. The force is known as Magnus force.

The knowledge of the Magnus force on a rugged sphere is also interesting in problems connected with transport of sand in rivers and channels, solid-liquid mixtures streams modelling, whereas a solid particle is approximated as a rugged sphere. Present paper deals with experimental investigation of Magnus force acting on a golf ball at Reynolds numbers corresponding to the sand transport in rivers and channels. The correspondence is achieved by using bigger model particles moving with lower velocities in the same fluid – in water. The drag force on a rotating golf ball is also investigated herein.

Davies (1949) investigated free falling rotating golf balls in a wind tunnel. Reynolds number based on the wind tunnel speed and the ball diameter $Re = \frac{ud}{\nu}$ was approximately $9 \cdot 10^4$, rotational Reynolds number $Re_\omega = \frac{r^2 \omega}{\nu}$ reached the values up to $2.5 \cdot 10^4$. Here d is the ball diameter, u is the ball velocity, ω is the angular velocity of the ball, ν is the fluid kinematic viscosity, r is the ball radius. From the drift of the balls he calculated the drag and the Magnus force. He noticed that for dimpled golf balls Magnus force should be much greater than that observed for smooth balls.

Briggs (1959) investigated the lateral deflection of a free falling and rotating baseballs and smooth spheres. He observed that the smooth ball deflected laterally opposite (reverse Magnus effect) in the direction to that of the baseballs, which

deflected in the direction according to the classical Magnus effect. Assuming that the lateral force during fall is a constant, and that the lateral deflection is much smaller than the total distance travelled by the ball, it is a simple matter to calculate the lateral Magnus force that acts on the ball. The experiments were conducted at $1.0 \cdot 10^5 \leq Re \leq 1.7 \cdot 10^5$ and $0.24 \leq \Gamma \leq 0.30$, where $\Gamma = \frac{r\omega}{u}$ is a spin parameter. The dimensionless numbers are bound as $\Gamma Re = 2Re_\omega$, and the motion of the ball can be determined by any pair of these numbers.

Bearman & Harvey (1976) measured the aerodynamical forces – drag and Magnus – on rotating and non-rotating golf balls in a wind tunnel with a wind tunnel balance. The balls of two types were used: with round dimples (conventional) and with hexagonal dimples. For the comparison with our experiments we used their data for the conventional golf ball. The measurements were done in ranges of dimensionless numbers $0.38 \cdot 10^5 < Re < 2.38 \cdot 10^5$, $0.02 \leq \Gamma \leq 0.3$. They indicated that at $Re > 1.26 \cdot 10^5$ the Magnus force coefficient C'_M and drag force coefficient C_d determined by formulae

$$F_M = C'_M \frac{1}{2} \rho_f S u^2, \quad (1)$$

$$F_d = C_d \frac{1}{2} \rho_f S u^2, \quad (2)$$

depend only on spin parameter Γ . Here F_M is the Magnus force, F_d is the drag force, S is a cross-sectional area of the ball, ρ_f is the water density. For lower Reynolds numbers the collapse of data was not observed.

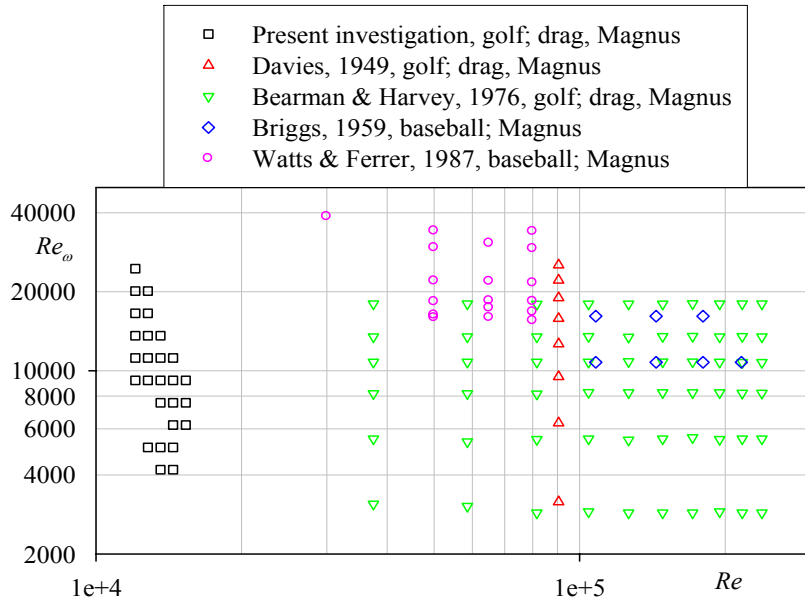


Figure 1. Map $Re \times Re_\omega$ of conducted experiments on Magnus force and drag force coefficients.

Watts & Ferrer (1987) measured with a strain gage the lateral force on a baseball in a wind tunnel. They indicate that the dimensionless coefficient C'_M depends only on a spin parameter Γ , and is not affected by the Reynolds number, though, later, Watts & Bahill (1990) noted, that the statement is not valid for the smooth spheres. The dimensionless numbers were $0.3 \cdot 10^5 < Re < 0.8 \cdot 10^5$, $0.4 < \Gamma < 1.6$.

The map $Re \times Re_\omega$ of conducted experiments is presented in Figure 1. For determining of the motion instant characteristics, we used here the $Re \times Re_\omega$ notation, instead of $Re \times \Gamma$, as most of other authors. That is done because the presumption, that the coefficients are influenced only by Γ , generally does not hold. Thus, for our research we found no motivation to mix rotational and translational velocities in a dimensionless number.

Experimental procedure

The experiments were carried out in a rectangular glass vessel 786 mm long, 602 mm wide and 990 mm high. The water depth was kept on the level 812 mm. The parameters of the used golf ball are presented in Table 1, the dimples of the ball surface were round. The temperature was about 20 °C, the water density was 1.00 g/cm³.

Table 1. The parameters of the golf ball

Mass, (±0.05g)	Volume, cm ³ ±0.05	Diameter, calculated from volume, cm	Density, g/cm ³
45.75	40.40	4.26	1.13

The hairlines were drawn on the ball to make possible the visualization of its rotation. The ball was speeded up in a special chute, ensuring the rotation in the plane of motion. The different initial heights of the ball at the chute and different inclinations of the chute were used to provide the different values of the translational and angular velocities of the ball motion.

The motion of the ball was recorded by a digital video camera. Video recording rate was 25 frames per second. The dimensions of obtained frames were 720x576 pixels. One pixel equalled approximately 2 mm in the plane of motion, the error of coordinate determination was one pixel.

From 23 to 32 images were recorded for a trajectory. From the images, the Cartesian coordinates $x(t)$, $y(t)$ of the ball centre and the angle of ball rotation $\varphi(t)$ as the functions of time, were read using the free software Graph2Digit. To evaluate the coordinates and the angle of revolution only trajectory segments close to straight lines were used; on those segments the motion of the ball was more or less quasi-steady. The non-steady process of entry into water was rejected as well.

Numerical method

For the quasi-steady process of 2D ball motion in fluid a steady approximation of drag force and drag moment acting on a spherical particle was considered. In the equations of motion we take into account the known unsteady forces, i.e. the history force and force of added mass, which are supposed to be small. Under such assumption the flow around the particle and hence the forces are completely determined by following set of parameters: ρ_f , μ , d , ω , u , where μ is the dynamic viscosity. Two dimensionless numbers, Re and Re_ω can be determined from the above mentioned parameters. Both

dimensionless coefficients – drag coefficient C_d and Magnus coefficient C_M , defined in (5), depend on these two numbers: $C_d = C_d(Re, Re_\omega)$ and $C_M = C_M(Re, Re_\omega)$, respectively. We define Magnus force coefficient somewhat otherwise than (1), with purpose to make the direction of Magnus force apparent from its definition.

According to Lukerchenko *et al.* (2005), the equation of the spherical particle translational motion is

$$\Omega\rho\frac{d\vec{u}}{dt} = \vec{F}_d + \vec{F}_g + \vec{F}_M + \vec{F}_H + \vec{F}_m, \quad (3)$$

where Ω is the particle volume, ρ is the particle density, and

$$\vec{F}_g = \Omega(\rho - \rho_f)\vec{g}, \quad (4)$$

$$\vec{F}_M = C_M \Omega \rho_f [\vec{\omega} \times \vec{u}], \quad (5)$$

$$\vec{F}_m = -C_m \Omega \rho_f \frac{d\vec{u}}{dt}, \quad (6)$$

$$\vec{F}_H = -6\pi\mu r \int_0^t \frac{d\vec{u}}{d\tau} K(t-\tau, \tau) d\tau, \quad (7)$$

where F_g , F_m , and F_H are the gravitational submerged force, the added mass force, the history force (Kim et al., 1998), respectively; \vec{g} is the gravity acceleration vector, C_M is the Magnus force coefficient and $C_m = 0.5$ is the dimensionless added mass coefficient. In history force integral

$$K(t-\tau, \tau) = \left\{ \left[\frac{\pi(t-\tau)v}{r^2} \right]^{1/(2C_1)} + G(\tau) \left[\frac{\pi |u(\tau)|^3 (t-\tau)^2}{2 rv f_H^3(Re(\tau))} \right]^{1/C_1} \right\}^{-C_1}, \quad (8)$$

where $C_1 = 2.5$, $f_H(Re) = 0.75 + C_2 Re(\tau)$, $C_2 = 0.126$, $G(\tau) = 1/\left(1 + \beta(\tau) \sqrt{M_1(\tau)}\right)$,

$$M_1 = \frac{2r}{u^2} \left| \frac{du}{dt} \right|, \quad \beta(\tau) = \frac{C_5}{1 + \phi(\tau) \phi(\tau)^{C_4} / \left[C_3 (\phi(\tau) + \phi(\tau)^{C_4}) \right]}, \quad C_3 = 0.07, \quad C_4 = 0.25,$$

$$C_5 = 22.0, \quad \phi(\tau) = \frac{M_2(\tau)}{M_1(\tau)}, \quad M_2 = \frac{(2r)^2}{u^3} \left| \frac{d^2 u}{dt^2} \right|. \quad \text{The expression for the history force with}$$

the kernel $K(t-\tau, \tau)$ proposed by Kim et al., 1998, is valid for Re up to 150, and particle to fluid density ratios from 5 to 200. For $Re \ll 1$ it makes the Basset expression for the history term, that was derived for a creeping flow. The conditions of the present experiments evidently do not satisfy the conditions of the history term validity. However, because of the lack of a more convenient expression, we used the aforementioned; on the other hand, in our experiments the force is small, due to the quasi-steadiness of the ball motion.

The forces acting on a particle and their orientation are shown in Figure 2. \vec{F}_d is directed oppositely to curve tangent unit vector $\vec{\tau}$, \vec{F}_M is parallel to curve normal unit vector \vec{n} . The values of coefficients C_d , and C_M can be calculated independently.

Since the scalar product of unit vector $\vec{\tau}$ and Magnus force \vec{F}_M equals zero, the Magnus force can be cancelled from (3), and the drag coefficient C_d can be expressed as

$$C_d = \frac{\left\{ \vec{F}_g + \vec{F}_H - \Omega(\rho + C_m \rho_f) \frac{d\vec{u}}{dt} \right\} \vec{\tau}}{\frac{\pi d^2}{4} \rho_f \frac{u^2}{2}}. \quad (9)$$

Similarly, multiplying (3) by \vec{n} the Magnus force coefficient C_M can be expressed:

$$C_M = \frac{\left\{ \Omega(\rho + C_m \rho_f) \frac{d\vec{u}}{dt} - \vec{F}_g - \vec{F}_H \right\} \vec{n}}{\Omega \rho_f [\vec{\omega} \times \vec{u}] \vec{n}}. \quad (10)$$

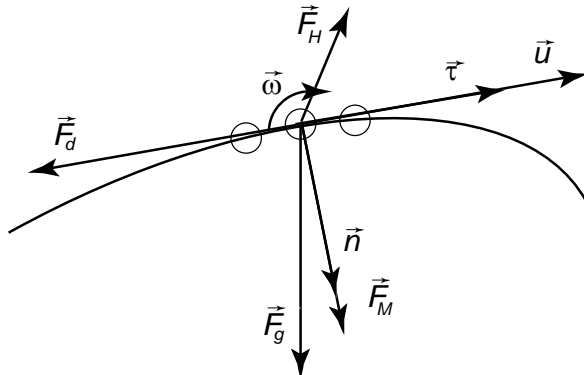


Figure 2 The forces acting on the rotating particle moving translationally in calm water.

The kernel of the history force integral has a singularity at the upper integration bound. Thus, for numerical calculation of the history force integral, an approximate method was used, similarly to that proposed by *Brush et al. (1964)* for calculation of the Basset force:

$$\begin{aligned} \int_0^t \frac{d\vec{u}}{d\tau} K(t-\tau, \tau) d\tau &= \int_0^{t-\Delta t} \frac{d\vec{u}}{d\tau} K d\tau + \int_{t-\Delta t}^t \frac{d\vec{u}}{d\tau} K d\tau \\ &\approx \int_0^{t-\Delta t} \frac{d\vec{u}}{d\tau} K d\tau + \frac{d\vec{u}}{dt} \int_{t-\Delta t}^t \left[\frac{\pi \mu}{r^2} (t-\tau) \right]^{-\frac{1}{2}} d\tau = \int_0^{t-\Delta t} \frac{d\vec{u}}{d\tau} K d\tau + \frac{d\vec{u}}{dt} \frac{r}{\sqrt{\pi \mu}} 2\sqrt{\Delta t}, \end{aligned} \quad (11)$$

where Δt is small.

Equations (9) and (10) allow the calculation of the dimensionless coefficients for each point of recorded particle trajectory, provided that the first and the second time-derivatives of the particle coordinates and of the angle of rotation are known. Before the first and the second derivatives were calculated, experimental data $x(t)$, $y(t)$ were fitted using the least square method with polynomial functions up to the third power of t , and $\varphi(t)$ was fitted with rational function $(a + t)/(b + ct)$. The used functions were chosen with the condition, that they should be simple and provide a good fit.

The drag force coefficient and the Magnus force coefficient were calculated numerically for each frame of a particle trajectory, except for the first two and the last two frames for which the second derivatives were not available. The corresponding values of Reynolds number Re and rotational Reynolds number Re_ω were also calculated for each frame of each particle motion record.

The following procedure was applied to average the experimental data. The experimental area Re vs. Re_ω ($1.2 \cdot 10^4 < Re < 1.6 \cdot 10^4$ and $3.8 \cdot 10^3 < Re_\omega < 2.7 \cdot 10^4$) was split into 5×10 cells, whose dimensions grow as geometric series. The use of geometric series for the length and width of a cell along Re and Re_ω axes makes the cells look uniform in logarithmic coordinates. For a cell, where at least four data points existed, C_d and C_M were calculated as an arithmetic mean of all data points in the cell. In most cases a cell comprised points from more than one trajectory. The positions of the individual cells were represented by the values of Re and Re_ω , which were the geometric mean of the values on the responsible boundary. The experimental data and the cells are illustrated in Figure 3.

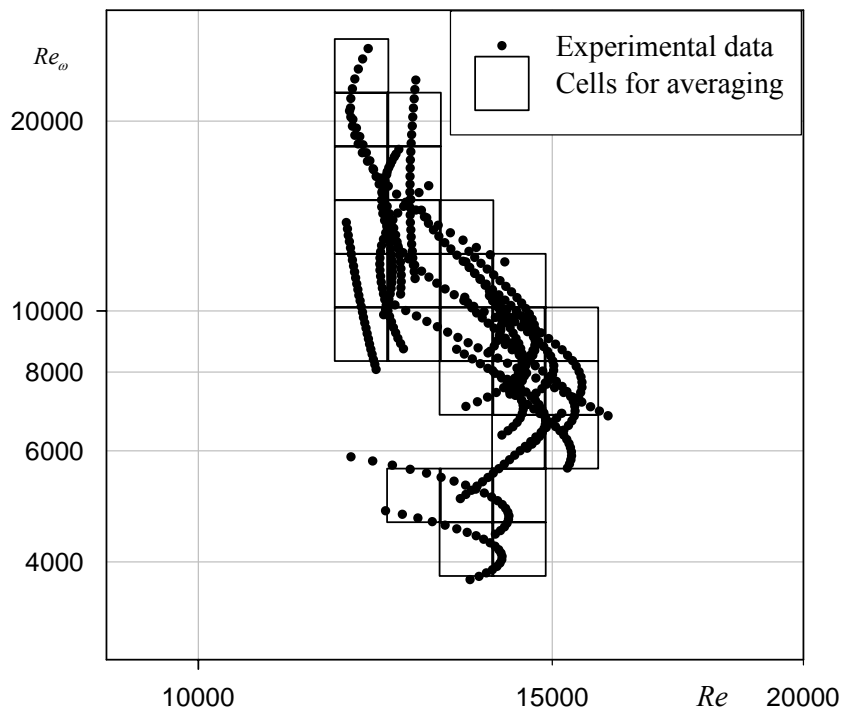


Figure 3 The $Re \times Re_\omega$ map of the experimental data and the cells.

Results

Calculated values of drag and Magnus coefficients with standard deviations versus Reynolds translational and rotational numbers are presented in Table 2. The average standard deviation for C_d is 6% and for C_M 12%, the values were in most cases computed from the data from different trajectories (see Figure 3), what means that the reproducibility of the experiments was good.

The plots of drag and Magnus coefficients compared with data of other authors are presented on Figures 4, 5. As can be seen from the comparison, the values of the coefficients and the tendencies are in a good accordance with data of other authors. Within the accuracy of such investigations, it can be said that the baseball results on Magnus force coefficient do not differ much from that of golf balls.

Table 2.

Re	Re_ω	C_d	ΔC_d	C_M	ΔC_M	Re	Re_ω	C_d	ΔC_d	C_M	ΔC_M
12057	9183	0.751	0.0126	0.130	0.0133	13596	7548	0.650	0.0652	0.124	0.0145
12057	11173	0.758	0.0406	0.112	0.0100	13596	9183	0.594	0.0478	0.117	0.0152
12057	13593	0.774	0.0370	0.092	0.0115	13596	11173	0.607	0.0540	0.103	0.0100
12057	16538	0.776	0.0305	0.073	0.0076	13596	13593	0.591	0.0692	0.082	0.0124
12057	20120	0.836	0.0233	0.055	0.0037	14438	4191	0.657	0.0232	0.099	0.0442
12057	24479	0.889	0.0067	0.043	0.0032	14438	5099	0.635	0.0344	0.120	0.0084
12804	5099	0.626	0.0065	0.074	0.0106	14438	6204	0.625	0.0342	0.096	0.0124
12804	9183	0.665	0.0282	0.106	0.0088	14438	7548	0.557	0.0360	0.128	0.0095
12804	11173	0.678	0.0410	0.106	0.0094	14438	9183	0.552	0.0326	0.123	0.0109
12804	13593	0.708	0.0608	0.091	0.0114	14438	11173	0.568	0.0490	0.110	0.0117
12804	16538	0.768	0.0688	0.072	0.0068	15332	6204	0.537	0.0330	0.116	0.0167
12804	20120	0.736	0.0052	0.055	0.0046	15332	7548	0.484	0.0409	0.122	0.0141
13596	4191	0.639	0.0495	0.065	0.0084	15332	9183	0.485	0.0157	0.126	0.0030
13596	5099	0.664	0.0611	0.115	0.0197						

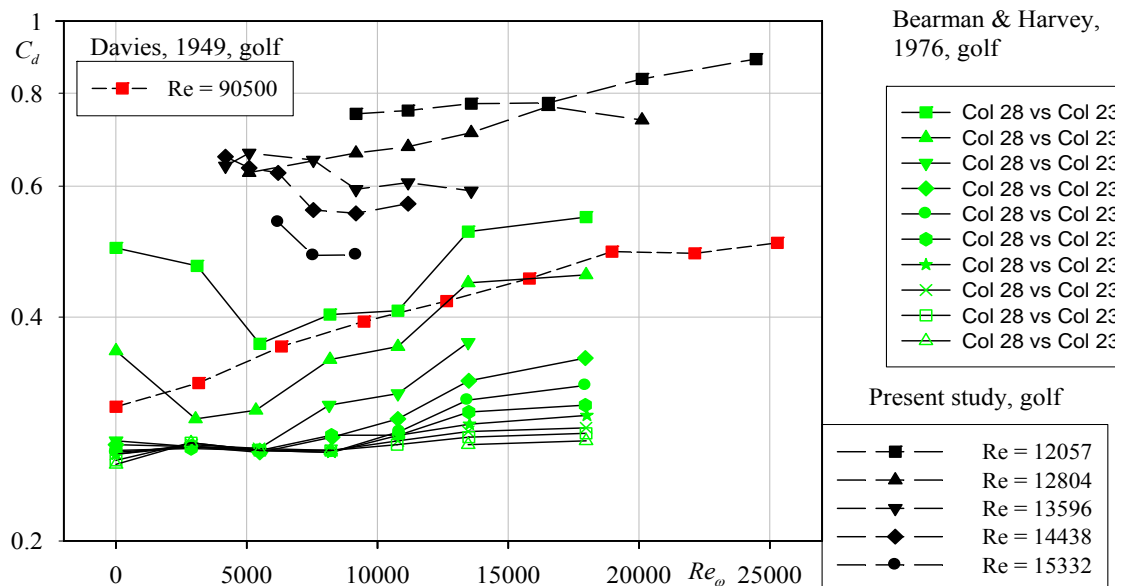


Figure 4 Drag force coefficient.

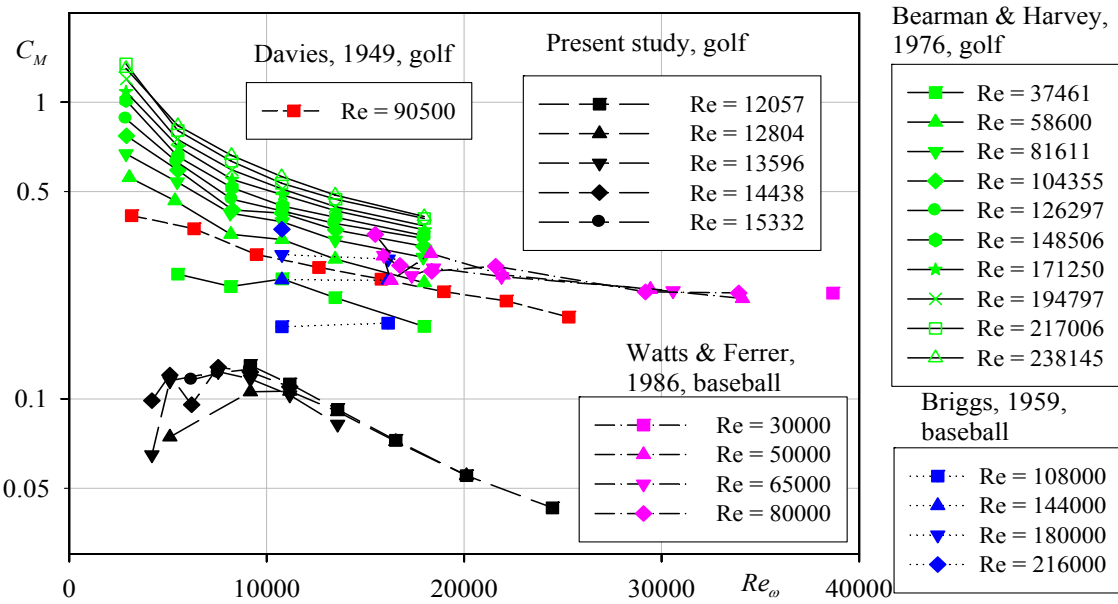


Figure 5 Magnus force coefficient.

Conclusions

The experimental investigation of the drag and Magnus forces on a golf ball moving translationally and simultaneously rotating in calm water was conducted. The motion of the ball during experiments was quasi-steady. The trajectories of the ball were recorded on a digital video-camera, and from them the coordinates of the ball motion were obtained.

The drag and the Magnus force coefficients were calculated numerically from the trajectories of the ball motion, by formulae (9), (10), that were obtained from equation of motion (3). The calculated data were averaged over rectangular cells on plane Re vs. Re_ω , $1.2 \cdot 10^4 < Re < 1.6 \cdot 10^4$ and $3.8 \cdot 10^3 < Re_\omega < 2.7 \cdot 10^4$. The coefficients were presented in tabulated form. They were found to be in satisfactory agreement with the coefficients measured by other authors in the adjacent ranges of Reynolds numbers, see Figures 4, 5.

Acknowledgements

The support under the project No. A200600603 of the Grant Agency of Academy of Sciences of the Czech Republic and under Institutional Research Plan No. AV0Z20600510 of Academy of Sciences of the Czech Republic is gratefully acknowledged.

Notation

C_d	- drag force coefficient;	Re_ω	- rotational Reynolds number;
C_m	- added mass coefficient;	S	- cross-sectional area of the ball;
C_M	- Magnus force coefficient;	t	- time;
d	- ball diameter;	u	- ball velocity;
F_d	- drag force;	$x(t), y(t)$	- coordinates of ball centre;

F_g	- gravitational submerged force;	$\varphi(t)$	- angle of ball rotation;
F_H	- history force;	Γ	- spin parameter;
F_m	- added mass force;	μ	- fluid dynamic viscosity;
F_M	- Magnus force;	ν	- fluid kinematic viscosity;
\vec{g}	- gravity acceleration vector;	ρ	- ball density;
\vec{n}	- normal to curve unit vector;	ρ_f	- water density;
r	- ball radius;	$\vec{\tau}$	- tangent to curve unit vector;
Re	- translational Reynolds number;	ω	- ball angular velocity;
		Ω	- ball volume.

References

- Bearman, P.W. & Harvey, J.K. (1976) Golf ball aerodynamics. *Aeronautical Quarterly*, May, pp. 112-122.
- Briggs, L.J. (1959) Effect of spin and speed on the lateral deflection(curve) of a Baseball; and the Magnus effect for smooth Spheres. *American Journal of Physics*, 27, pp. 589-596.
- Brush, L.M. Jr., Hau-Wong Ho & Ben-Chie Yen (1964) Accelerated motion of a sphere in a viscous fluid. *J. Hydraul. Division, Proc. of ASCE*, 90, No. HY1, pp. 149-160.
- Davies, J. M. (1949) The aerodynamics of golf balls. *J. Appl. Phys.*, 20, pp. 821-828.
- Lukerchenko, N., Kharlamov, A., Kvurt, Yu., Chara, Z., & Vlasak, P. (2005) Experimental evaluation of the Magnus force coefficient of the rotating spherical particle. *Proc. Int. Conf. IM 2005*, Svatka, Czech Republic.
- Kim, I., Elghobashi, S., & Sirignano, W.A. (1998) On the equation for spherical-particle motion: effect of Reynolds and acceleration numbers. *J. Fluid Mech.*, 367, pp. 221-253.
- Watts, R.G. & Bahill, A.T. (1990) Keep your eye on the ball: the science and folklore of baseball. *W.H. Freeman and Company*, NY.
- Watts, R.G. & Ferrer, R. (1987) The lateral force on a spinning sphere: Aerodynamics of a curveball. *Am. J. Phys.*, 55 (1), pp. 40-44.